Biogenesis of hepatitis B virus e antigen is driven by translocon-associated protein complex and regulated by conserved cysteine residues within its signal peptide sequence

Helena Zábranská, Aleš Zábranský, Barbora Lubyová, Jan Hodek, Alena Křenková, Martin Hubálek, Jan Weber and Iva Pichová (iD)

Institute of Organic Chemistry and Biochemistry of the Czech Academy of Sciences, Prague, Czech Republic

Hepatitis B virus uses e antigen (HBe), which is dispensable for virus infectivity, to modulate host immune responses and achieve viral persistence in human hepatocytes. The HBe precursor (p25) is directed to the endoplasmic reticulum (ER), where cleavage of the signal peptide (sp) gives rise to the first processing product, p22. P22 can be retro-translocated back to the cytosol or enter the secretory pathway and undergo a second cleavage event, resulting in secreted p17 (HBe). Here, we report that translocation of p25 to the ER is promoted by translocon-associated protein complex. We have found that p25 is not completely translocated into the ER; a fraction of p25 is phosphorylated and remains in the cytoplasm and nucleus. Within the p25 sp sequence, we have identified three cysteine residues that control the efficiency of sp cleavage and contribute to proper subcellular distribution of the precore pool.

Introduction

Hepatitis B is a liver infection caused by the hepatitis B virus (HBV), which can induce both acute and chronic disease and is a major global health problem. According to the World Health Organisation, an estimated 296 million people worldwide are infected with HBV. HBV, a member of the family Hepadnaviridae, is a small enveloped DNA virus with a genome containing only four open reading frames (C, P, S and X) that largely overlap and encode multiple proteins using different in-frame start codons [1,2]. For example, the HBV preC-C gene gives rise to two different products translated from distinct mRNAs – core protein (HBc) and precore protein (HBe). Despite their high sequence similarity, these proteins exhibit different functions and subcellular localisations. HBc is a cytosolic protein with a molecular weight of 21 kDa responsible for the assembly of icosahedral viral particles and pregenomic RNA encapsidation. On the other hand, the precore precursor, which includes the entire core-protein sequence, undergoes a two-step maturation process resulting in the production of the extracellular immunomodulatory HBe antigen [3–6].

Precore is translated with a 29-amino-acid N-terminal sequence that leads this 25-kDa protein (p25)

into the endoplasmic reticulum (ER), where the signal peptide (sp) comprising the first 19 amino acids (also denoted as the pre-sequence) is cleaved off, producing a 22-kDa precore protein (p22) [7]. The remaining 10-amino-acid extension at the p22 N-terminus, termed precore propeptide (pro-sequence), is not present in the core protein and plays a crucial role in precore folding. An intrasubunit disulphide bond between Cys −7 within the propeptide sequence and Cys 61 changes the dimerisation interface, prevents multimerisation and holds the protein in a dimeric state [8–10]. The majority of p22 is further processed at its C-terminus by furin protease in the trans-Golgi network, giving rise to mature HBe antigen (p17). The mature antigen is secreted [11–14] and performs an immunomodulatory function in the establishment of persistent infection [15–18]. Interestingly, a certain portion of the precore protein is secreted with sp still attached as PreC protein, but the biogenesis and function of this protein have yet to be elucidated [19–21].

However, approximately 15–20% of p22 does not enter the secretory pathway and is retrotranslocated back to the cytosol and transported into the nucleus [22–25]. A certain portion of the cytosolic p22 becomes phosphorylated (p22^p) [22]. The biological function of the precore protein in the cytoplasm and nucleus remains poorly understood. P22 can form heterodimers with the core protein and destabilise the viral particle, which may negatively regulate viral infection [26]. Conditional expression of the precore protein may alter the expression profile of several host genes in transfected hepatocytes [27]. Precore may also influence the Rab-7-dependent regulation of HBV secretion [28], promote hepatocellular carcinogenesis by affecting the stability and activity of the p53 tumour suppressor [29] and influence the antiviral signalling of IFN-α [30]. Recently, precore protein has also been shown to affect HBsAg expression [25].

The mechanism by which p22 is distributed to different cellular compartments remains unclear. The Sec61 translocon, together with associated protein complexes, serves as a crossroad for protein translocation into the ER and in some cases also for export via the ER-associated protein degradation (ERAD) pathway (reviewed in Ref. [31]). This machinery with the participation of Derlin-1 protein has already been shown to play a role in the retrotransport of p22 from ER to the cytosol by employing one of ERAD members, the ER-resident chaperone GRP78/BiP [24]. GRP78/BiP participates not only in binding the proteins subjected to ERAD but also in mediating translocon gating [32–34]. Another factor that can support protein translocation and Sec61 translocon channel

opening in a substrate-specific manner is the translocon-associated protein complex (TRAP), which consists of four subunits (α, β, γ, δ) and supports Sec61 gating for proteins with weak signal sequences [35–37].

Despite recent progress in understanding the intracellular pathways of individual precore forms and growing evidence for their specific roles, many aspects of cytosolic p25 and p22 protein function remain unclear. Furthermore, the mechanism that determines the distribution of precore forms to the secretory or retrotranslocation pathways is not understood. Here, we reveal that conserved Cys residues in the sp sequence are critical for the rate of p25 processing and appear to serve as an auto-regulating factor that influences the intracellular localisation of the precore. We also describe how the host factor TRAP promotes efficient precore protein ER translocation and prevents mislocalisation.

Results

A fraction of the cytosolic p25 precursor is phosphorylated

To investigate in detail the process of precore maturation, we performed ^{35}S metabolic labelling of cells transiently transfected with an HBe-producing construct (pCEP HBeM1A, the resulting protein denoted as HBe or precore wt), in which the internal ATG initiation triplet for the core protein (HBc) was mutated (Met/Ala mutation in position 1) (Fig. 1). All experiments were initially performed in HEK293T cells and then verified in hepatoma cell lines – Huh7 or HepG2-hNTCP cells. Metabolic labelling was mostly performed in Huh7 cells because this cell line had generally provided a higher signal of the precore protein and a lower level of the radioactive background than transfected HepG2-hNTCP cells. In HBV-infected hepatocytes, the lower expression level of precore protein did not allow the detection of p25 precursor and also the presence of core protein complicated the HBe analysis. We performed ELISA to determine the difference in the expression levels of HBe secreted from pCEP-HBeM1A-transfected and HBV-infected HepG2-NTCP cells. The amount of HBe produced by plasmid-transfected cells within 24 h was approximately 90 times higher than that secreted from the infected cells (data not shown).

Transfected Huh7 cells were labelled for 30 min, lysed and HBV precore-related proteins were immunoprecipitated with anti-core polyclonal antibody. Although the HBe sample was dominated by p22, we
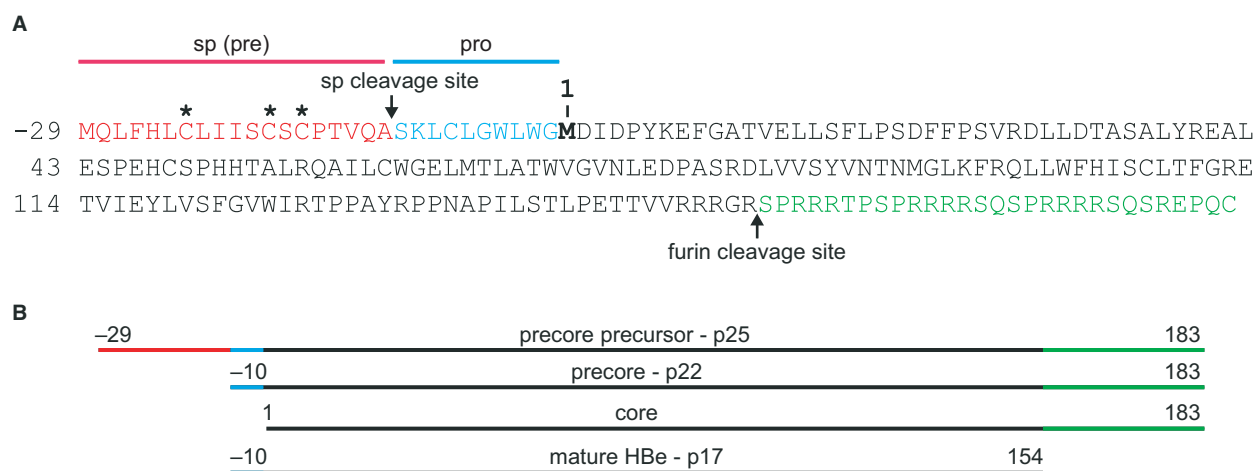
A

B

Fig. 1. HBV precore precursor and related protein products. (A) A sequence of the precore precursor p25. The cysteine residues at positions −23, −18 and −16 are marked by asterisks. The initial methionine of the core protein in position 1 is labelled in bold, and the sites of signal-peptide (sp) cleavage and p17 proteolytic maturation are indicated with arrows. (B) A schematic representation of individual preC/C gene products.

also observed (in agreement with other groups [22,25,38]) a significant portion of unprocessed p25 (around 30% of the total precore signal in pulse samples for wt) (Fig. 2A), indicating that either translocation to the ER or sp cleavage was not 100% efficient. Furthermore, p25 appeared as a double band, suggesting that a portion of it was post-translationally modified (Fig. 2A).

Since both HBV core and p22 are known to be phosphorylated [39,40], we have investigated the possibility that the upper p25 band (denoted as p25^p) represents an un-translocated version of p25 that is phosphorylated in the cytoplasm. The treatment of the immunoprecipitated samples of precore proteins with λ-protein phosphatase (λ-PP) resulted in the disappearance of the p25^p form, accompanied by the enrichment of p25 as visualised by autoradiography (Fig. 2A). These data demonstrate that a portion of p25 is not translocated to the ER and becomes phosphorylated in cytosol.

To analyse the detection of individual HBV core-related proteins, we compared their gel-mobility pattern in different cell lines. We transiently transfected HEK 293T cells and HepG2-hNTCP cells with appropriate DNA constructs – pcDNA3 HBc (encoding HBV core, p21), pCEP HBeM1A Δsp (encoding a precore protein without the signal peptide and enabling the expression of the cytosolic phosphorylated version of the HBV precore protein, p22^p) and pCEP HBeM1A. Cells were isotopically pulse-labelled for 30 min in the presence of ^{35}S, and core-related proteins were immunoprecipitated with anti-core

polyclonal antibody. A half of each immunoprecipitated sample was treated with λ-PP. The specific mobility pattern in 15% SDS/PAGE gel is shown for each construct (Fig. 2B). In samples derived from the HEK293T cell, we have been able to distinguish between phosphorylated and non-phosphorylated versions of all p21, p22 and p25 proteins. The pattern does not substantially differ between HepG2-hNTCP and HEK293T cells except for the p25^p protein, migrating as a sharper band in the sample derived from HEK293T cells than in the sample from HepG2-hNTCP cells (similar to the one observed for HBe in Huh7 cells, Fig. 2A).

Mutation of Cys residues in the signal peptide of p25 stimulates its cleavage and enhances the rate of p17 biogenesis

Since our experiments indicated delayed the processing or ineffective translocation of p25, we sought to define the factors that influence the trafficking pathway of the HBV precore precursor. The N-terminal sp sequence of p25, which contains three Cys residues at positions −16, −18 and −23, directs the protein into the ER (Fig. 1). While Cys −7 within the propeptide sequence is known to stabilise the intrasubunit dimer via a disulphide bond with Cys 61, the role of the three Cys residues located within the sp sequence had long remained unclear [9]. We first examined whether the p25 maturation process was influenced by changes in redox conditions. Huh7 cells transfected with pCEP HBeM1A were labelled for 30 min with ^{35}S in the

presence or absence of 5 mM DTT. The cells were harvested and lysates were subjected to immunoprecipitation with anti-core antibody. In Huh7 cells cultivated without a reducing agent, we observed all intracellular precore forms: p25^p, p25 and p22. In DTT-treated cells, however, the sp was almost completely removed and p22 was predominant (Fig. 2C). On the other hand, DTT is known to induce ER stress, which may cause some differences in the maturation pattern.

To address the contribution of the Cys residues in the sp sequence to p25 processing, we substituted these cysteines with alanines (the construct pCEP HBeM1A C-16A, C-18A, C-23A; the resulting protein is denoted as HBe3CA). The expression of this construct was performed in Huh7 cells labelled for 30 min with ^{35}S 24 h after transfection. The autoradiographs of immunoprecipitated proteins (Fig. 2D) indicate that the processing of the HBe3CA unphosphorylated precursor was more effective; we observed only phosphorylated p25^p and p22 and did not detect any p25. The treatment of these immunoprecipitates with λ-PP resulted in the disappearance of the p25^p band, further confirming the presence of only the phosphorylated form of p25 in cells transfected with the HBe3CA construct. The fuzzy phosphorylation pattern of p25 in Huh7 cells did not allow us to calculate the ratio of p25/p25^p during the pulse period in transfected cells. Nevertheless, after the evaluation of the p22 and p25+p25^p signal of three independent experiments, we observed the enrichment of p22 species in HBe3CA samples as compared to the wt. On the other hand, the analysis of

samples from HEK293T cells enabled the separation of p25 and p25^p, making it possible to measure the intensity of individual p22, p25 and p25^p bands. The decrease of the p25 signal of HBe3CA is compensated for by a proportional increase in the p22 level (Fig. 2E).

To analyse the contribution of the conserved sp Cys residues to the rate of p25 processing and p17 release, we performed pulse/chase experiments with both wt HBe and the HBe3CA mutant. Huh7 cells were isotopically pulse-labelled for 30 min in the presence of ^{35}S and chased at different time points. HBV precore-related proteins were immunoprecipitated with anti-core polyclonal antibody (Fig. 2F). In cells producing wt HBe as well as the HBe3CA construct, the amount of p22 appeared to be substantially reduced after approximately 4 h of chase, which was in good agreement with increased extracellular p17 concentration at this time point. In the media, we also detected the PreC protein, representing the p17 with unprocessed sp. In cells producing the HBe3CA mutant, p17 secretion was not impaired, demonstrating that the mutation of Cys residues does not interfere with sp function. Moreover, we observed neither the unprocessed unphosphorylated p25 protein in these cells nor the PreC protein in the medium, suggesting more efficient sp cleavage than for the wt.

To explore the function of the N-terminal sequence of the precore precursor in the context of the whole virus, mutations of Cys −16, −18 and −23 of p25 were introduced into the HBV recombinant cccDNA

Fig. 2. An analysis of p25 protein phosphorylation and the effect of the mutation of Cys residues in the sp sequence on HBV precore-protein processing and virus infectivity. (A) Huh7 cells expressing HBV precore precursor were metabolically labelled for 30 min with ^{35}S, lysed and subjected to immunoprecipitation with anti-core antibody. The immunoprecipitated samples were untreated (−) or treated (+) with λ protein phosphatase and separated by SDS/PAGE. The electrophoretic mobility of precore-related proteins was analysed by autoradiography. The migration positions of the HBV precore forms p25^p, p25 and p22 are indicated. (B) A comparison of the electrophoretic mobility of core- and precore-related proteins. HEK293T and HepG2-hNTCP cells expressing HBV core (p21), precore Δsp (p22) and precore precursor (p25) were metabolically labelled for 30 min with ^{35}S, lysed and subjected to immunoprecipitation with anti-core antibody. The electrophoretic mobility of precore-related proteins was analysed by autoradiography. (C) The ratios of individual precore-protein forms produced in the presence (+) or absence (−) of DTT. Huh7 cells expressing the precore precursor were metabolically labelled for 30 min with ^{35}S under standard or reducing (5 mM DTT) conditions. HBV precore-derived proteins were immunoprecipitated from the harvested cells with anti-core antibody, separated by SDS/PAGE, and analysed by autoradiography. (D) Precore-related forms of HBe and the HBe3CA mutant. The experiment was performed as for A; the phosphorylation of HBe3CA p25 protein was demonstrated by λ-PP treatment. (E) The relative ratio of individual precore-protein forms detected in Huh7 cells and HEK293T cells. Protein signals were evaluated from three independent pulse experiments. The intensity of p22 and p25 signals was quantified by QUANTIMAGE software and expressed as relative proportions of the total intracellular precore-signal level, the error bars indicate the standard deviation. (F) Pulse-chase analysis of precore-protein processing and secretion. Huh7 cells expressing HBe or HBe3CA proteins were metabolically labelled for 30 min with ^{35}S, and then chased for 0.5, 1, and 4 h. At all time points, both cells and media were harvested and subjected to immunoprecipitation with anti-core antibody. Proteins were separated by SDS/PAGE and analysed by autoradiography. (G) A comparison of HBe secretion by cells infected with wild-type and mutant precore rcccDNA. HepG2-hNTCP cells in 12-well plates were infected in triplicate with wild-type rcccDNA (wt rcccDNA) and mutant precore rcccDNA (HBe3CA rcccDNA) with an equal MOI of 2000 VGE/cell. HBe secretion in the culture supernatants was determined by ELISA on days 0, 3, 6 and 14. The data are plotted as the mean ± SEM of three biological replicates, *P* obtained by a two-tailed paired *t* test, *n* = 3.
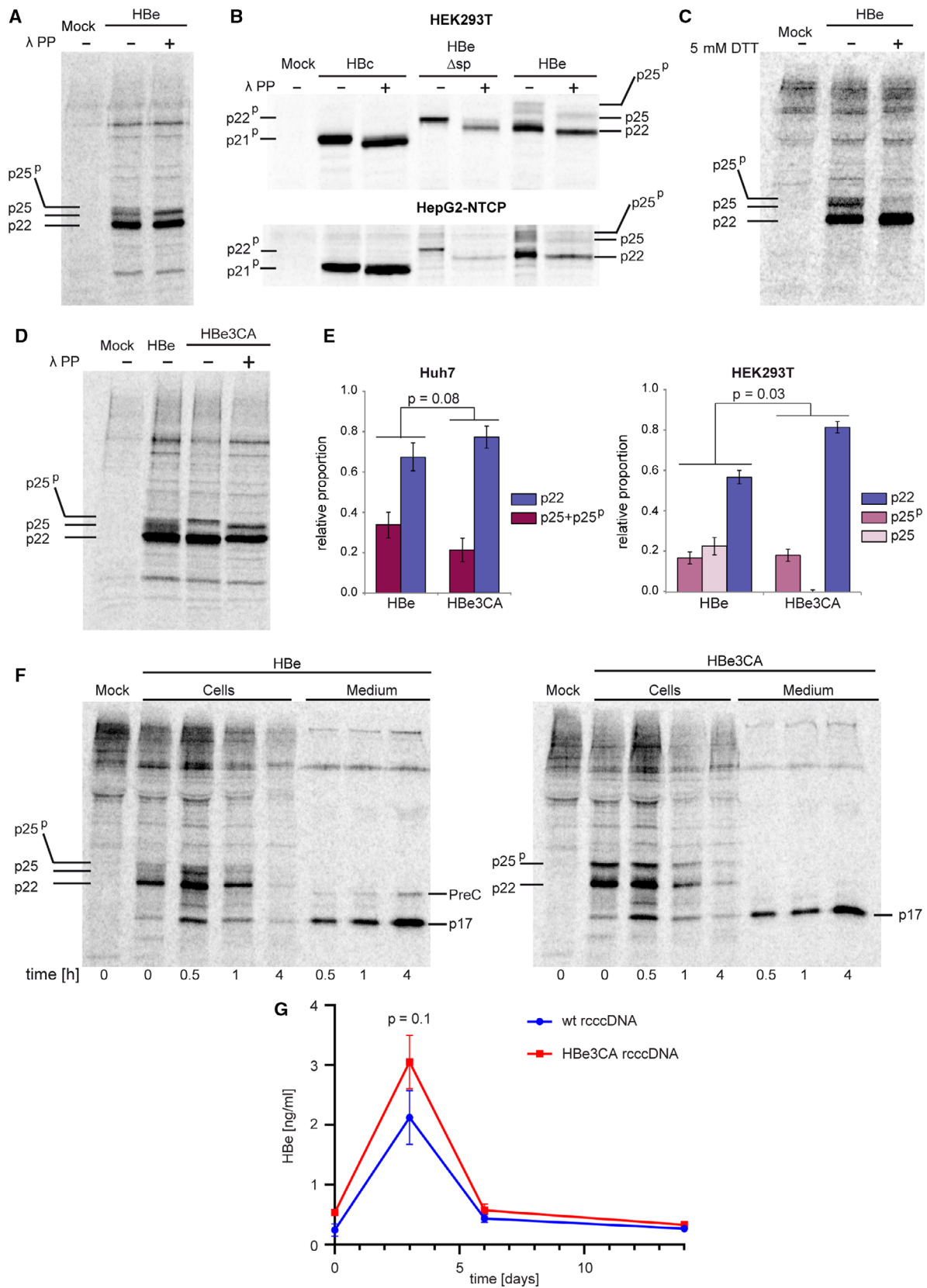
```
HBeAg_HBV   MQ--------------LFHLCLIISC-SCPTVQASKLCLGWLWGM...
HBeAg_ASHV  MY--------------LFHLCLVFACVSCPTVQASKLCLGWLWDM...
HBeAg_WHV1  MY--------------LFHLCLVFACVPCPTVQASKLCLGWLWGM...
HBeAg_DHBV  MWNLRITPLSFGAACQGIFTSTLLLSCVTVPLVCT--IVYDSCLYM...
```

Fig. 3. Alignment of signal-peptide sequences of precore proteins from different hepadnaviruses. Conserved cysteines in the signal-peptide sequence are highlighted in red, green and blue; the initial methionine of the core protein is in bold. HBV, hepatitis B virus (GenBank: BAJ51641.1); ASHV, arctic squirrel hepatitis virus (GenBank: Q64896); WHV, woodchuck hepatitis virus (GenBank: P0C6J2); DHBV, duck hepatitis B virus (GenBank: P0C6J9). Sequences were aligned using CLUSTAL OMEGA tool (https://www.ebi.ac.uk/Tools/msa/clustalo).

minichromosome (3CA rcccDNA). After the transfection of wt or 3CA rcccDNAs into HepG2-hNTCP cells, the wt and C3A virions were purified from the culture medium. Subsequently, HepG2-hNTCP cells were infected with wt and 3CA HBV virions (MOI = 2000 VGE/cell) and the rates of HBeAg expression and secretion were determined by ELISA on days 0, 3, 6 and 14 post-infection. Both wt and 3CA viruses were able to infect HepG2-hNTCP, but the 3CA mutant virus appeared to yield higher levels of p17 in the media than the wt virus (Fig. 2G). This implies that 3CA mutation may lead to more efficient maturation and secretion of the precore protein.

These results indicate a regulatory role of the N-terminal Cys residues, that are conserved among hepadnaviruses (Fig. 3) in HBV precore-protein maturation and consequently in the rate of p17 secretion.

Cysteine residues in the sp sequence influence subcellular localisation of the precore protein

To determine the localisation of individual precore-protein forms, we performed crude subcellular fractionation of HEK 293T cells, which yielded better separation of individual fractions than Huh7 cells. The cells were transfected with the pCEP HBeM1A or pCEP HBeM1A 3CA construct and isotopically labelled for 30 min with ^{35}S. Individual cytosolic, microsomal and nuclear fractions of the cell lysates were isolated and verified by western blots using antibodies against specific organelle markers (Fig. 4).

Precore-related proteins were immunoprecipitated with anti-core polyclonal antibody and visualised by autoradiography. Autoradiographs of HBe samples showed that not only unphosphorylated p22 but also full-length p25 were preferentially localised in microsomes (Fig. 4A), once again indicating inefficient and likely post-translational sp cleavage. On the contrary, the microsomal fraction of HBe3CA samples contained almost no p25, demonstrating a very fast and effective N-terminal truncation process of this mutant. To determine whether the inefficient cleavage of wt p25 and its presence in the microsomal fraction are a consequence of a translocation defect and whether the full-length precursor is only attached to the surface of microsomes, we subjected this fraction to proteinase K (PK) cleavage. A sample with 1% Triton 100 added to dissolve all membranes served as a control. After 1 h incubation of microsomes with PK, we still detected undigested wt p25, indicating its membrane shielding and functional translocation (Fig. 4B). The phosphorylated p25^p form was present in both the cytosolic fraction and nuclear extract (Fig. 4C). Individual cellular fractions were evaluated by western-blot analysis using antibodies against specific markers of organelles (Fig. 4D). Since it is difficult to immunoprecipitate specifically isotopically labelled proteins from the nuclear pellet because of the high background signal, we analysed nuclear fractions (extract and pellet) by western blot (Fig. 4E). Although the sensitivity of this approach did not allow us to distinguish between p25 and p25^p, we could clearly detect the enrichment of

Fig. 4. Subcellular localisation of wt HBe and HBe3CA-derived precore forms. (A) An autoradiograph of ^{35}S-labelled proteins immunoprecipitated with anti-core antibody. HEK 293T cells producing HBe or HBe3CA proteins were labelled for 30 min, lysed (total lysate, TL) and subjected to subcellular fractionation. Precore-related proteins from individual fractions representing cytosol (Cyt.), nuclear extract (Nu.Ex.) and microsomes (Mic.) were immunoprecipitated, separated by SDS/PAGE, and visualised by autoradiography. (B) Immunoprecipitated microsomal fractions from HEK 293T cells were treated with proteinase K and analysed by autoradiography. (C) Precore-related proteins immunoprecipitated from a nuclear extract of HEK 293T cells were treated with λ-PP separated by SDS/PAGE. The electrophoretic mobility of samples untreated (−) or treated (+) with λ-PP was analysed by autoradiography. (D) The evaluation of individual cytosolic, microsomal and nuclear fractions of the cell lysate by western-blot analysis using antibodies against specific markers of organelles. PDI, protein disulphide isomerase A1. The dashed line indicates separated parts of the same membrane. (E) Analysis of microsomal fraction, nuclear extract and nuclear pellet by western blot using anti-HBV core antibody and specific markers of organelles.
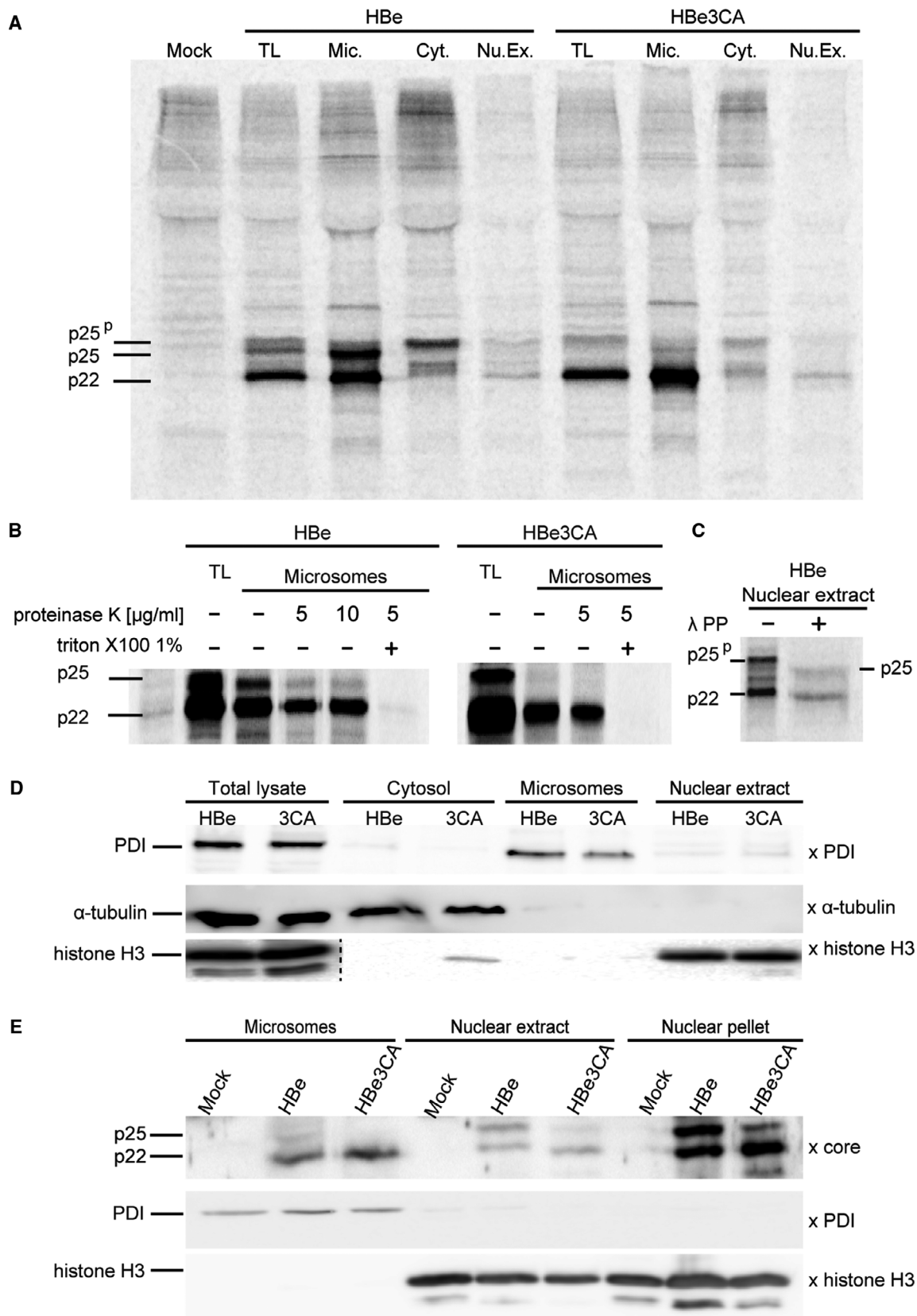
the p25 precursor signal in the wt sample in comparison with the 3CA mutant.

The subcellular localisations of C-terminally HA-tagged wt HBe, the HBe3CA mutant and HBc protein (control) were evaluated by immunofluorescence analysis (IFA) using anti-HA antibody (Fig. 5) in transfected HEK 293T cells. Whereas the wt precore protein was localised exclusively in the cytoplasm and the core protein was distributed between the cytosol and the nucleus with predominantly nuclear localisation, the HBe3CA mutant displayed a mixed phenotype. We observed cells with a cytoplasmic phenotype resembling that of wt, as well as cells exhibiting both a nuclear and cytoplasmic distribution pattern (28% of the total number of 200 evaluated cells). We assume that the increased level of HBe3CA mutant in the nucleus is related to a higher intracellular level of p22, resulting from faster sp processing, which could contribute to the massive retro-translocation from the ER.

Taken together, these data indicate that precore-protein translocation is a controlled process, in which the delay in p25 N-terminal cleavage and thus the regulation of the p22 level prevent its mislocalisation within cells. Cys residues in the sp sequence are likely key factors in this sequential HBe maturation.

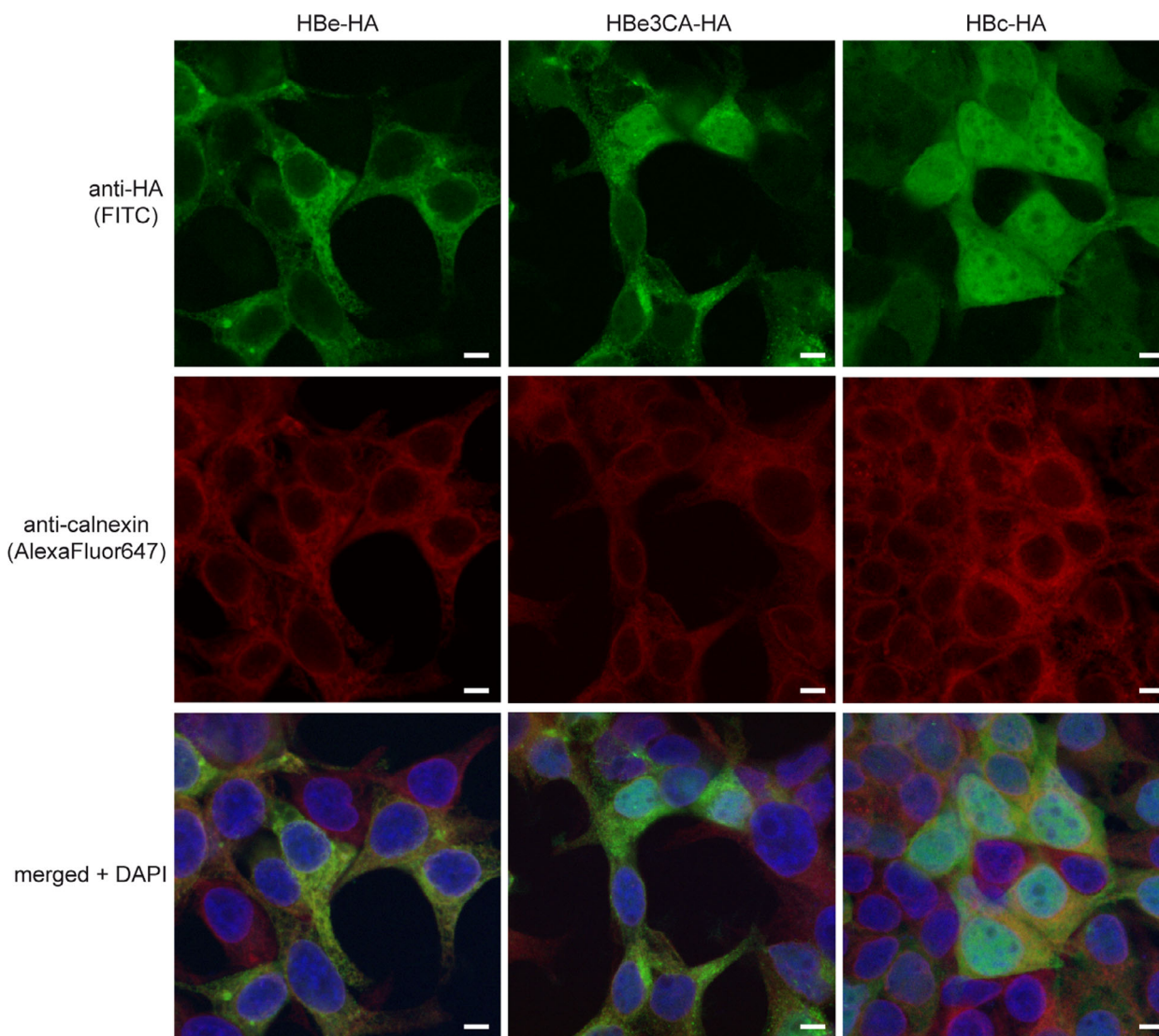**Fig. 5.** Subcellular distribution of wt HBe and HBe3CA-derived precore forms. Representative confocal-microscopy images of C-terminally HA-tagged HBe, HBe3CA and HBc visualised by FITC-conjugated anti-HA antibody in transfected HEK 293T cells. The ER is stained with anti-calnexin AlexaFluor647-conjugated antibody. Calnexin (red), HBe, HBe3CA, HBc (green) and DAPI (blue). The scale bar represents 5 µm.

The HBV precore precursor interacts with TRAP

To identify the host proteins potentially involved in the translocation of the HBV precore protein, we performed HBe interactome analysis using an LC-MS/MS-based proteomics approach. To block HBe secretion and thereby enhance its detection in cell lysates, we added Brefeldin A, which inhibits protein transport from the ER to the Golgi complex. HepG2-hNTCP cells transfected with a plasmid encoding C-terminally HA-tagged HBe or HBe3CA were cultivated for 36 h, treated with Brefeldin A for 4 h and harvested. Cell lysates were subjected to immunoprecipitation using anti-HA magnetic beads, and recovered proteins were analysed by LC-MS/MS for identification and label-free quantification (LFQ). Triplicates of HBe (or HBe3CA) and control cell lines allowed the application of a Student's *t*-test statistically to determine the proteins specifically enriched in HBe positive samples. The result of the analysis is shown in the volcano plot (Fig. 6).

Among the proteins enriched in samples containing HBe (or HBe3CA), we identified the previously described precore interacting partners C1qBP, GRP78/BiP [24,41] and protein kinase SRPK1, which mediates

HBV core phosphorylation [42]. In both HBe-HA and HBe3CA-HA samples, we also repeatedly observed peptides derived from the Sec61 translocon complex and subunits (α, β, δ) of TRAP, an accessory component that triggers Sec61 channel opening in a substrate-specific manner [43]. No significant differences were observed between wt precore and the 3CA mutant with regards to detected co-immunoprecipitated proteins.

To evaluate potential interactions between the HBV precore protein and the TRAP complex, we co-transfected HEK 293T cells with the C-terminally HA-tagged HBe construct and individual C-myc-tagged TRAP subunits α, β, γ and δ and performed pull-down experiments using anti-HA magnetic beads followed by western-blot evaluation using anti-c-myc antibody (Fig. 7A). We detected a significant signal corresponding to all four individual TRAP subunits after co-immunoprecipitation with the HBe construct, indicating a mutual interaction between the HBV precore and the TRAP. In control samples transfected with mock DNA and individual TRAP subunits, we observed a non-specific interaction between TRAP β and the magnetic beads; the other three subunits did not display any nonspecific background. The
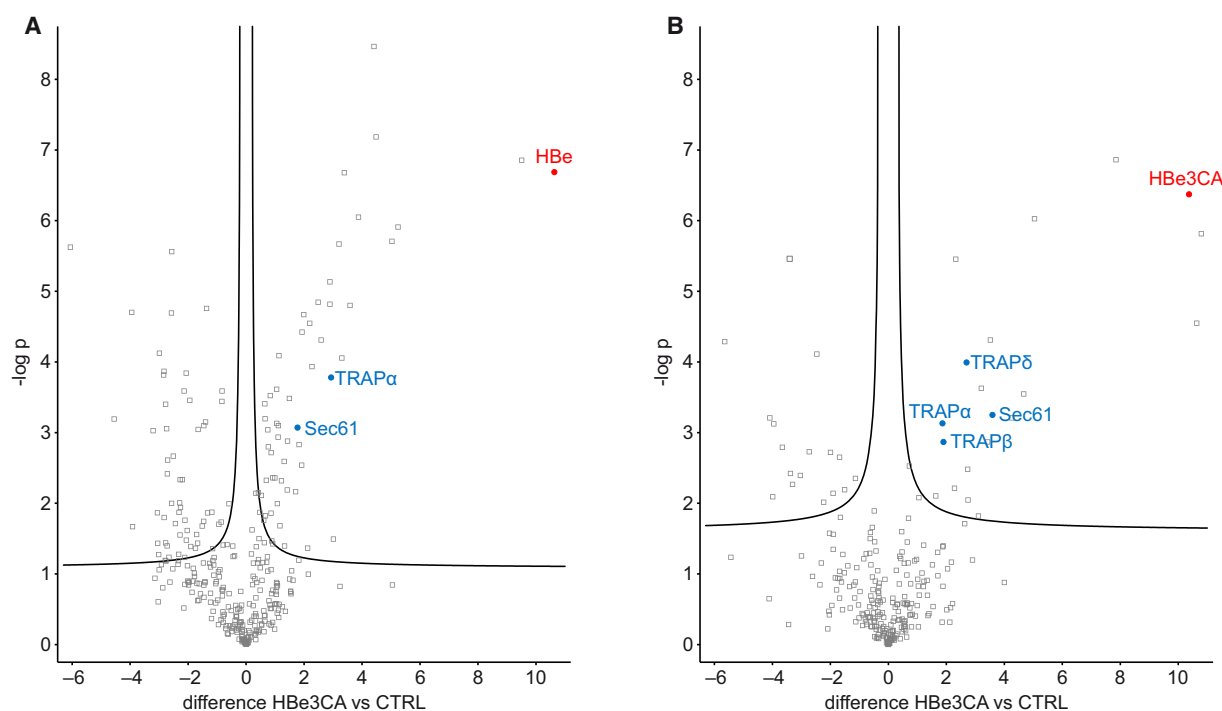
Fig. 6. Volcano plots as a result of student's *t*-test comparison of shotgun LC-MS/MS analysis of proteins co-immunoprecipitated with HBe-HA (A) and HBe3CA-HA (B) expressed in HEPG2-hNTCP cells. The scatter plot shows differential patterns between the HBe or HBe3CA sample and a negative control sample (CTRL, empty vector) performed in biological triplicates. The blue points in the plot represent Sec61 and TRAP complex subunits, and the red dot represents a bait protein.

repeatedly confirmed association between the HBV precore protein and TRAP-complex subunits strongly implies the involvement of TRAP in the translocon gating of p25 protein.

The TRAP complex cooperates in the translocation and sequential maturation of the HBV precore protein

To investigate whether the TRAP complex is involved in precore-protein translocation into the ER, siRNA-mediated knockdown of either the α or δ subunit was performed in HEK 293T cells. The cells were co-transfected with a plasmid producing HBe and siRNA targeting one TRAP subunit (α or δ). Metabolic labelling followed by a pulse-chase experiment (30 min pulse, 3 h chase) was performed 48 h after the transfection. The efficiency of silencing was confirmed by western blot using monoclonal antibodies that recognise the TRAP α or δ subunit (Fig. 7B) and evaluated by the QUANTIMAGE software (GE Healthcare, Chicago, IL, USA). In three independent experiments, the silencing of TRAP α reached the average of 81% ($P < 0.05$), the silencing of the TRAP δ subunit 78% ($P < 0.05$). Cell lysates and the collected medium were immunoprecipitated using polyclonal anti-HBV core antibody. The remarkable effect of TRAP depletion became evident at the intracellular precore-protein level. In cells producing wt precore protein with the silencing of either the TRAP α or δ subunits, the signals of p22 and p25 significantly decreased as compared to nondepleted cells and were restored after the addition of the proteasome inhibitor MG132. The effect was stronger upon TRAP δ knockdown (Fig. 7C). In the medium of cells overexpressing the HBV precore with TRAP silencing, we observed slightly lower levels of mature p17 secretion, again especially in samples with TRAP-δ depletion (Fig. 7D). Our

results indicate that the silencing of individual TRAP subunits promotes the degradation of HBe wt, presumably due to ineffective translocation.
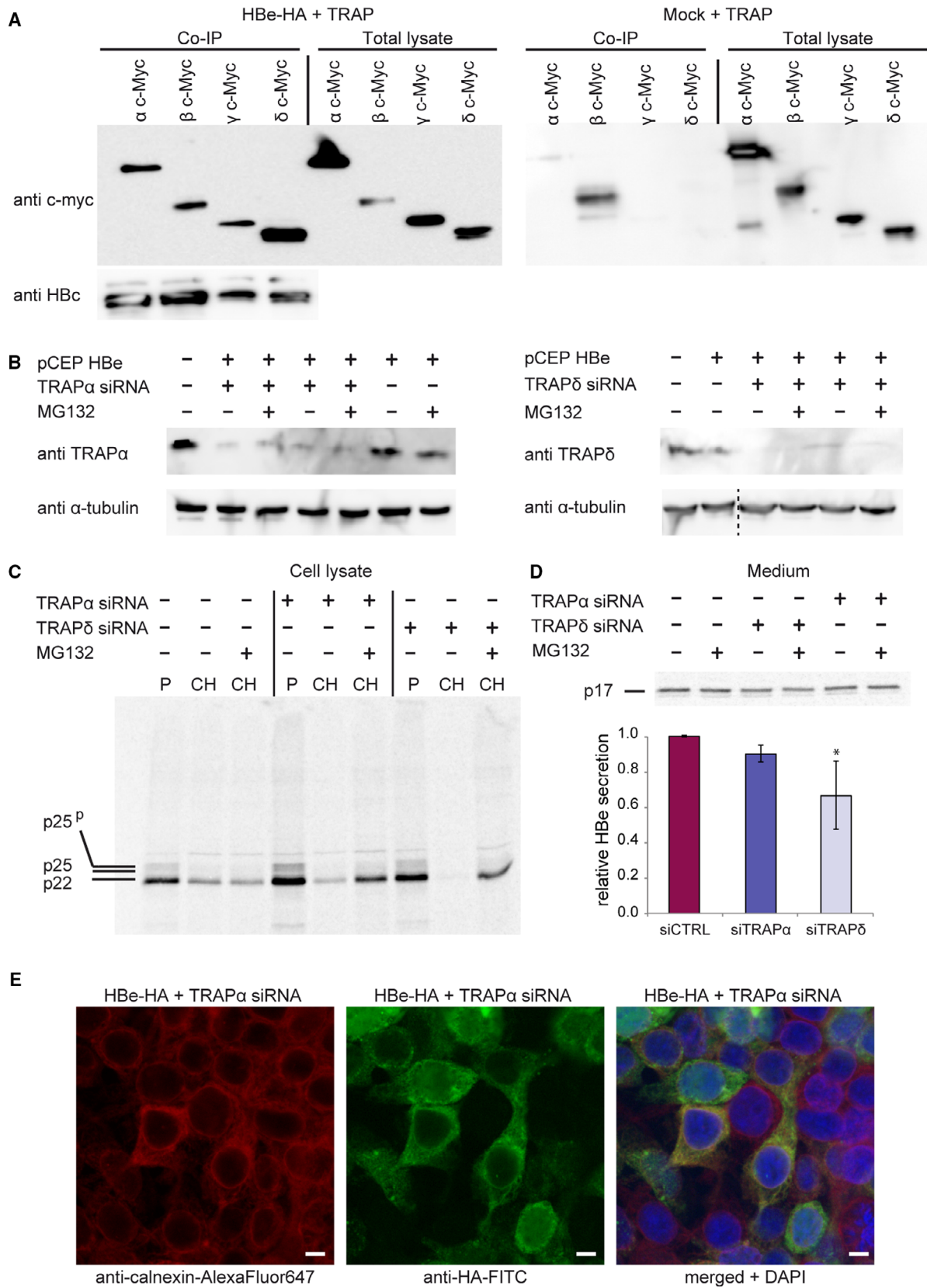
Next, we analysed the effect of TRAP depletion on the subcellular distribution of the precore protein. HEK 293T cells were co-transfected with the HBe-HA producing construct and either TRAP α- or δ-targeting siRNA and examined by confocal microscopy after immunofluorescence staining using anti-HA antibody conjugated with FITC (Fig. 7E). In both TRAP-silenced samples, the typical ER localisation pattern of the precore protein was disrupted in a fraction of the cells (24% for TRAP α-silenced cells, 200 cells evaluated). The protein appeared to be distributed between the cytoplasm and the nucleus, indicating a certain degree of malfunction in the translocation process.

It is evident that the leader sequence of the HBe p25 precursor is too weak to mediate an autonomous translocation into ER and that the assistance of the TRAP complex in conducting channel gating is indispensable for proper HBV precore subcellular localisation and p17 biogenesis.

The silencing of individual TRAP-complex subunits in HBV-infected cells reduces the extracellular level of HBe

To determine whether the TRAP complex mediates the co-translational translocation of the HBe precursor in HBV-infected hepatocytes, we examined the consequences of the siRNA-mediated knockdown of TRAP subunits in HepG2-hNTCP cells. The siRNA-treated HBV-infected hepatocytes were cultured for 5 days before HBe secretion was determined by ELISA. In comparison with HBe secretion following knockdown with non-targeting siRNA, the targeting of the α, β

Fig. 7. Co-immunoprecipitation of the HBV precore protein with individual TRAP subunits and the TRAP-depletion effect on precore stability and translocation. (A) HEK 293T cells were co-transfected with an HA-tagged HBe-producing construct (or mock DNA) and plasmids expressing individual c-myc-tagged TRAP subunits. The precore protein was immunoprecipitated with anti-HA magnetic beads and the samples were analysed by western blot using anti c-myc antibody to detect interacting TRAP proteins. (B) HEK 293T cells were co-transfected with an HBe-producing construct and siRNAs targeting either TRAP α or δ genes. The silencing effect was evaluated by western-blot analysis. The dashed line indicates separated parts of the same membrane. (C) Knockdown of TRAP decreases the efficiency of HBe secretion. Forty-eight hours after transfection, TRAP-silenced cells were metabolically labelled for 30 min with ^{35}S (P) and chased for 4 h (CH) with or without the addition of the proteasome inhibitor MG132. The cells and media were harvested and subjected to immunoprecipitation with anti-core antibody. The proteins were separated by SDS/PAGE and analysed by autoradiography. (D) The signal intensity of p17 in the medium was quantified and shown relative to the unsilenced sample. The bars represent the averages of three independent experiments, whereas the error bars indicate the standard deviation, * denotes a significance level ≤ 0.05. (E) Representative confocal-microscopy images of HA-tagged HBe in HEK 293T cells depleted for the TRAP α subunit visualised by FITC-conjugated anti-HA antibody; the ER is stained with anti-calnexin AlexaFluor647-conjugated antibody. Calnexin (red), HBe, HBc (green) and DAPI (blue). The scale bar represents 5 μm.

A

HBe-HA + TRAP

Mock + TRAP

B

C

Cell lysate

D

Medium

E

anti-calnexin-AlexaFluor647   anti-HA-FITC   merged + DAPI

and δ TRAP subunits by siRNAs reduced the extracellular level of HBe (Fig. 8A). In contrast, the level of the HBs antigen secreted from TRAP-silenced cells remained comparable to that from non-silenced cells (Fig. 8B). These results indicate that the stability of TRAP is dependent on the presence of all its components and that the efficiency of HBe secretion is reduced upon the downregulation of TRAP in HBV-infected cells. The efficiency of silencing was monitored by RT-qPCR 3 days after transfection (Fig. 8C).

To exclude the possible cytotoxic effect of individual knockdowns, we analysed the general effect of TRAP silencing on cell viability. HepG2-hNTCP cells were transfected with individual siRNAs, and we included 5% DMSO as a positive control. After 5 days of incubation, cell viability was determined by XTT assay in biological triplicates (Fig. 8D). Other than slightly reduced metabolic viability in cells treated with TRAPδ siRNA, no significant changes were observed.
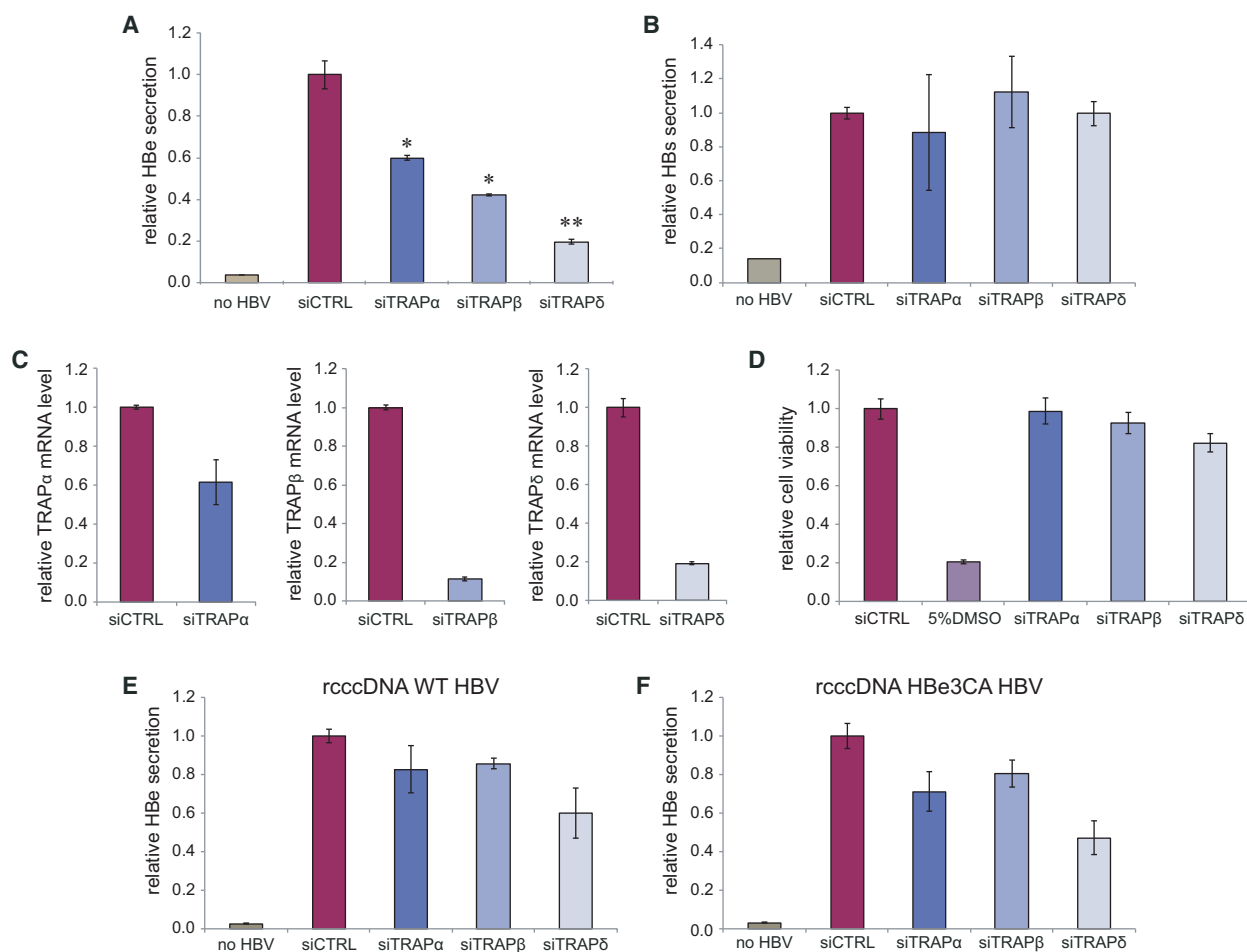

Fig. 8. The depletion of TRAP subunits downregulates the extracellular level of HBe but not HBs in HBV-infected hepatocytes. Biological triplicates of HepG2-hNTCP cells were first transfected with siRNA oligonucleotides for 24 h, then infected with HBV at a MOI of 1500 VGE/cell for another 96 h before the cells and media were harvested. Secreted HBe (A) and HBs (B) antigens in the media were quantified by ELISA. The error bars represent standard deviations. The asterisks indicate statistically significant differences between the control (siCTRL) and the respective depleted TRAP subunit determined by ANOVA (*$P < 0.05$; **$P < 0.01$). The data are representative of three biological replicates. (C) Knockdown efficiency was verified by RT-qPCR following total RNA isolation from the cells harvested 3 days after transfection. (D) The cytotoxic effect of the silencing was evaluated by XTT assay 5 days after transfection. TRAP-subunit knockdown affects HBe secretion for both wt (E) and mutant HBe3CA (F) HBV. HepG2-hNTCP cells were simultaneously transfected with rcccDNA plasmid coding for either WT or HBe3CA virus and siRNAs targeting individual TRAP subunits. Secreted HBe levels in the media were quantified by ELISA after 5 days of cultivation.

To determine possible differences between HBe and HBe3CA regarding TRAP depletion in HBV-producing cells, we co-transfected HepG2-hNTCP cells with HBV rcccDNA (containing either HBe or HBe3CA genes) and siRNAs targeting individual TRAP subunits. The resulting level of mature p17 secretion was evaluated by ELISA after 5 days. In this experimental setup, we observed reduced HBe levels in the media of TRAP-depleted cells for both wt rcccDNA (Fig. 8E) and HBe3CA rcccDNA (Fig. 8F).

Discussion

By closely examining the maturation of the HBe precursor p25, we demonstrate here that the HBV precore protein is present in cells in different forms and is localised to different subcellular compartments. We identified the unprocessed p25 precursor in microsomes and its phosphorylated form (p25^p) in the cytosol and nucleus. We found that the three Cys residues in positions −16, −18, and −23 play a coordinated regulatory role that contributes to proper p25 processing and localisation. Furthermore, our results illustrate the importance of the host TRAP complex for HBV precore-precursor ER translocation.

The phosphorylation and dephosphorylation of the HBV core protein play a crucial role in the assembly, disassembly and nuclear localisation of capsids [44–48]. The nuclear localisation of HBc has been associated with two co-dependent nuclear localisation signals within the arginine-rich domain [49,50], which by analogy are also present at the C-terminus of the precore (p25 and p22). The nuclear localisation of phosphorylated p22 has been described [40,51]; our results have revealed that the phosphorylated version of p25 also is localised in the nuclear fraction of mammalian cells, although its role in the nucleus has yet to be elucidated. Locarnini *et al.* [27] have observed that the precore protein induces repression of many genes in transfected hepatocytes and behaves like a tumour-suppressing protein with anti-apoptotic activity. However, this observation has been presented as a general effect of precore expression in cells, and no particular activity has been attributed to individual forms of the precore protein.

The factors involved in retaining a significant portion of p25 in the cytoplasm or causing the retro-translocation of p25 from the ER membrane back to the cytosol also remain poorly understood. Our findings show that the addition of a reducing agent (DTT) into cell-culture media or mutations of three Cys residues in the sp sequence accelerate p25 processing and lead to an almost complete conversion of p25 to p22. Four cysteines in the N-terminal part of p25 are conserved among hepadnaviruses, and their function in the viral life cycle has not been established. Wasenauer *et al.* [52] have reported that these Cys residues are dispensable for mature HBe production. In agreement with their data, we found that the replacement of three cysteines in the sp sequence with alanines did not abolish precore maturation. The sp function of the HBe3CA construct remained unchanged, and the mutated protein was translocated into the ER. Single-round infectivity assays revealed a slightly higher signal of mature p17 secreted from HepG2-hNTCP cells infected with HBe3CA HBV particles in comparison with cells infected with the wt HBV genome. Interestingly, confocal-microscopy experiments have shown that Cys residues in the sp are responsible for the proper precore-localisation pattern and prevent the spread of the precore across the cell in a core-like phenotype. It appears that HBV needs to regulate the precore-precursor maturation process tightly to avoid unfavourable p22 localisation and its possible interference with core functions. The controlled maturation also allows the interplay between the core and precore proteins, which seems to be important for HBeAg expression [25]. Additionally, the distribution of the dual p25 population (phosphorylated in cytosol and nucleus, nonphosphorylated in microsomes) must be under some control mechanism. Several ER-resident proteins, such as calreticulin, have another independent role in cytosol, and their segregation between compartments is influenced by the weak ability of their signal sequences to mediate translocation [53,54]. Our results have shown that p25 processing and localisation are regulated by the conserved Cys residues within the sp. In the co-translational pathway, the translocation process is initiated during protein synthesis when the sp is recognised by SRP. As long as this sequence is sufficiently hydrophobic and helical (so-called 'strong'), it can facilitate translocon opening. The tertiary folding is delayed until the protein exits the channel and enters the ER lumen (reviewed in Ref. [55]). Domains folded prematurely in the cytosol inhibit translocation [56,57]. The gating of proteins with 'weak' signal sequences is postponed, and their interactions with additional Sec61 accessory proteins such as TRAM, TRAP, Sec62/63 or BiP are needed (reviewed in Ref. [58]). Apparently, the sp of the HBV precore protein is not strong enough to open the translocon channel, and a host chaperone is employed to mediate successful gating or to stabilise the binary Sec61–p25 complex. This hypothesis is in agreement with the observation that p25 displays impaired sp cleavage in a non-mammalian model, possibly caused by a lack of appropriate cellular partners [12,38].

Our work establishes the TRAP complex as a novel interacting partner participating in p25 translocation. After the siRNA-mediated knockdown of the TRAP complex, the translocation of wt precore-protein precursor is disrupted, and the protein is directed to proteasomal degradation. In HBV-infected hepatocytes, this is reflected in significantly decreased production of secreted p17. Several signal sequences, including those of the prion protein and preproinsulin, require the TRAP complex for successful protein-conducting channel opening [59,60]. It has been proposed that low hydrophobicity and high GP content are common features for most signal sequences of TRAP clients [43]. Interestingly, instead of a GP-rich patch, the primary structure of the sp of HBV p25 contains three conserved cysteines, which seem to be involved in the autoregulation of HBe biogenesis. Their precise role and possible participation in tertiary structure still need to be elucidated, but evidently, they are not indispensable for TRAP interaction and the facilitation of translocon gating. Instead, they are more likely responsible for the moderation of the translocation process and thus its regulation.

In summary, we present evidence that the three conserved Cys residues in the sp of the HBV precore precursor p25 serve as an auto-regulatory factor controlling proper progression of the precore-translocation process and thus preventing the mislocalisation of the precore. We have also identified the TRAP complex as a host factor required for successful translocon gating of p25 and for the support of mature p17 biogenesis.

Materials and methods

DNA constructs

HBV precore- and core-coding sequences were derived from the HBV genome-containing plasmid pHBV4.1 (genotype D, serotype *adw*) obtained from PhD Huiling Yang (Gilead Sciences, Foster City, CA, USA). The HBV core protein-coding region was amplified using the forward primer 5′-ATCATAAGCTTACCATGGACATCGACCCTTATAAAG-3′ and the reverse primer 5′-TAGATGGTACCCTAACATTGAGGTTCCCGAG-3′ and subcloned into the pcDNA3.1 vector (Clontech, Mountain View, CA, USA) via *Hind*III and *Kpn*I restriction sites, giving rise to the construct pcDNA3 HBc. The precore-precursor gene was amplified using the forward primer 5′-ATCTAAAGCTTACCATGCAACTTTTTCACCTCT-3′ and the reverse primer 5′-TAGATGGATCCCTAACATTGAGGTTCCCGAG-3′ and introduced into the pCEP vector (Invitrogen, Carlsbad, CA, USA) via *Hind*III and *Bam*HI restriction

sites. To remove the initiating ATG codon for the HBV core protein, an M1A mutation was introduced by site-directed Pfu mutagenesis using the mutagenic primers 5′-TGGCTTTGGGGCGCCGACATTGACC-3′ and 5′-GGTCAATGTCGGCGCCCCAAAGCCA-3′, giving rise to the construct pCEP HBeM1A.

The C-terminal HA tag was introduced into the pCEPH-BeM1A construct using the reverse primer 5′-AGCTCGGATCCTCAAGCGTAGTCCGGGACGTCGTAAGGGTAACATTGAGGTTCCCGAG-3′. The following forward primer was used for the mutation of three cysteines at positions −23, −18 and −16 of the precore signal-peptide sequence to give rise to the construct pCEP HBeM1A3CA: 5′-ATCTAAAGCTTACCATGCAACTTTTTCACCTCGCCCTAATCATCTCTGCTTCAGCTCCTACTGTTCAAGC-3′.

The minicircle-producing plasmid for wt HBV recombinant cccDNA (*wt* rcccDNA) was kindly provided by P. Chen (Shenzhen Institutes of Advanced Technology, Chinese Academy of Sciences, Shenzhen, China) [61]. The rcccDNA plasmid designated as C3A rcccDNA, which carries a triple C-to-A mutation in the precore ORF at positions −16, −18 and −23, was generated by site-directed mutagenesis (QuikChange II XL Site-Directed Mutagenesis Kit; Agilent Technologies, Santa Clara, CA, USA) with three subsequent rounds of PCR using the following primers: C1A-F, 5′-GCGATGCAACTTTTTCCTAATCATCACCTCGCCTCTTGTTCATG-3′; C1A-R, 5′-CATGAACAAGAGATGATTAGGGCGAGGTGAAAAAGTTGCATCGC-3′; C2A-F, 5′-CCATGCAACTTTTTCACCTCGCTCTAATCATCTCTGCTTCAG-3′; C2A-R, 5′-CTGAAGCAGAGATGATTAGAGCGAGGTGAAAAAGTTGCATGG-3′; C3A-F, 5′-CAACTTTTTCACCTCGCCCTAATCATCTCTGCTTCAGCTCCTACTGTTCAAGCC-3′; C3A-R, 5′-GGCTTGAACAGTAGGAGCTGAAGCAGAGATGATTAGGGCGAGGTGAAAAAGTTG-3′.

The constructs of individual c-myc-tagged human TRAP subunits (α, β, δ) under the CMV promotor were purchased from OriGene Technologies (Rockville, MD, USA; #RC202408, #RC213580, #RC201079, # C201593).

rcccDNA production and purification

The wt and C3A mutant rcccDNA plasmids were transformed into the *Escherichia coli* strain ZYCY10P3S2T, and the rcccDNA was isolated using the MC-Easy minicircle production kit (System Biosciences, Palo Alto, CA, USA) according to the manufacturer's recommendations.

siRNA

SiRNAs targeting individual hTRAP subunits (α, β, γ, δ) were purchased from Santa Cruz Biotechnology (SCBT, Dallas, TX, USA; # sc-63153, #sc-63147, #sc-63148, #sc-63149).

Antibodies

The rabbit polyclonal anti-HBV core-protein antiserum was obtained after the immunisation of three animals with 1.4 mg·mL^{-1} purified denatured (boiling in 1% SDS, 0.1 M DTT) HBV core protein produced in *E. coli* (Moravian Biotech, Brno, Czech Republic). Mouse monoclonal antibodies against individual human TRAP subunits were purchased from SCBT (#sc-373916, #sc-517428, #sc-376706). Antibodies for IFA include anti-HA antibody conjugated with FITC (Sigma-Aldrich, St. Louis, MO, USA; #H7411) and anti-calnexin conjugated with AlexaFluor647 (Abcam, Cambridge, Great Britain; #ab225062).

Cells

HEK 293T (human embryonic kidney cell line; ATCC, Manassas, VA, USA) and Huh7 cells (differentiated hepatocyte-derived carcinoma cell line, Japanese Collection of Research Bioresources Cell Bank, Ibaraki, Osaka, Japan) were cultured in Dulbecco's Modified Eagle Medium (DMEM) supplemented with 10% FBS (VWR, Radnor, PA, USA) and an antibiotic mixture [penicillin/streptomycin (PenStrep); Sigma-Aldrich] at 37 °C in a 5% CO_2 atmosphere.

HepG2-hNTCP, a HepG2 human liver cancer cell line stably transfected with the human HBV entry receptor (sodium taurocholate co-transporting polypeptide, NTCP), was obtained from S. Urban (Heidelberg University Hospital, Heidelberg, Germany). The cells were cultured in DMEM supplemented with 10% FBS, the antibiotic mixture (PenStrep), and puromycin (0.05 mg·mL^{-1}; Sigma-Aldrich) at 37 °C in a 5% CO_2 atmosphere.

Cell-proliferation assay

The labelling reagents XTT (sodium 3′-[1-(phenylaminocarbonyl)-3,4-tetrazolium]-bis (4-methoxy6-nitro) benzene sulfonic acid hydrate) and PMS (*N*-methyl dibenzopyrazine methyl sulphate) were purchased from Sigma-Aldrich. The assay was performed according to the protocol in Cell Proliferation Kit II (XTT) (Roche, Basel, Switzerland; #11 465 015 001).

Transfection

According to the respective manufacturer's instructions, plasmid DNA was introduced into HepG2-hNTCP cells using the Lipofectamine™ 3000 Transfection Reagent (ThermoFisher Scientific, Waltham, MA, USA), Huh7 cells were transfected with GenJet™ (SignaGen Laboratories, Rockville, MD, USA), and HEK 293T cells were transfected with a 1 : 3 ratio of DNA : polyethylenimine (PEI, 25 kDa linear; Sigma-Aldrich). The transfection of siRNA was performed using the X-tremeGENE siRNA

Transfection Reagent (Roche) for HEK 293T cells and Lipofectamine RNAiMAX Transfection Reagent (Thermo-Fisher Scientific) for HepG2-hNTCP cells, according to the manufacturers' protocols.

RT-qPCR

The intracellular levels of mRNA for TRAP-complex subunits were estimated by RT-qPCR using the Luna Universal One-Step RT-qPCR Kit (NEB, Ipswich, MA, USA) following total RNA isolation with the RNeasy Mini Kit (Qiagen, Hilden, Germany). Primers targeting TRAPα, β and δ mRNAs were purchased from SCBT (#sc-63153-PR, #sc-63147-PR, #sc-63148-PR). The samples were analysed as technical duplicates.

Metabolic labelling and pulse/chase analysis

Confluent Huh7 or HEK 293T cells grown on 60-mm dishes were starved 18 h after transfection with DMEM lacking cysteine and methionine for 15 min, pulsed for 30 min with 10 μCi [^{35}S]-labelling mix (Trans^{35}S-Label™ MP Biomedicals, Irvine, CA, USA) and subsequently chased with the complete DMEM medium for the desired time periods. The harvested cells were lysed in lysis buffer A (1% Triton X-100, 50 mM of NaCl, 1% deoxycholate, 25 mM of Tris, pH 8) containing 1 mM of PMSF and Complete™ EDTA-free protease-inhibitor cocktail (Roche). The nuclei were removed by centrifugation for 1 min at 3000 *g*, and immunoprecipitation of the precleared lysate was performed using polyclonal anti-core antibody and protein A sepharose beads (Invitrogen). The immunoprecipitated complexes were washed twice in buffer B (1% Triton X-100, 50 mM of NaCl, 1% deoxycholate, 0.1% SDS, 25 mM of Tris, pH 8) and once in 20 mM of Tris, pH 8. Sepharose beads were resuspended in SDS/PAGE loading buffer and boiled for 5 min. Proteins were separated on 15% SDS/PAGE and subjected to phosphorimager analysis. Signal intensity was evaluated using QUANTIMAGE software (GE Healthcare, Chicago, IL, USA).

Immunofluorescence analysis

Transiently transfected HEK 293T cells were grown on 22-mm glass coverslips for 24 h, briefly washed with PBS and fixed with 4% paraformaldehyde in PBS at room temperature for 30 min. The fixed cells were washed with PBS and permeabilised with 0.2% Triton X-100 in PBS for 30 min. The permeabilised cells were immunostained in PBS, 0.2% Triton X-100, 10% FBS for 1 h using anti-HA and anti-calnexin antibodies. The cells were washed three times for 10 min with 0.2% Triton X-100 in PBS. The immunostained coverslips were mounted on slides in ProLong Diamond Antifade Mountant with DAPI (ThermoFisher Scientific). Images were acquired with a three-dimensional

Zeiss LSM 780 microscopy system (Carl Zeiss, Oberkochen, Germany) using a 63× oil objective with a numerical aperture of 1.4. The images were collected with a pinhole of 0.7 μm in diameter (1 Airy unit), averaged four times and processed with ZEN 2011 software (Carl Zeiss).

Crude subcellular fractionation

Fractionation was performed according to the protocol described by Holden and Horton [62] with slight modifications. Transfected cells grown in 100-mm plates were labelled for 30 min with ^{35}S and subsequently washed with PBS and detached with 1 mL of trypsin. Trypsin was quenched by the addition of 2 mL of ice-cold complete DMEM media with 10% FBS. Cells were centrifuged for 1 min at 4 °C and 200 g. The supernatant was aspirated and the cells were washed with ice-cold PBS. The collected cells were resuspended in 5 mL of ice-cold lysis buffer 1 [150 mM of NaCl, 50 mM of HEPES, pH 7.4, 25 μg·mL^{-1} of digitonin (Sigma-Aldrich)], incubated for 10 min at 4 °C, and centrifuged for 10 min at 10 000 g (step 1). The supernatant was mixed with 500 μL of Triton X-114, kept on ice for 1 h, heated at 37 °C for 3 min and centrifuged 3000 g at room temperature for 3 min. The upper aqueous phase contained the purified cytosolic fraction. The pellet from step 1 was washed in cold PBS, resuspended in 5 mL of buffer 2 (150 mM of NaCl, 50 mM of HEPES, pH 7.4, 1% NP40), incubated on ice for 30 min and centrifuged at 2000 g for 10 min. The resulting supernatant contained the microsomal fraction. The pellet was resuspended in 2 mL of buffer 3 [150 mM of NaCl, 50 mM of HEPES, pH 7.4, 0.1% SDS, 0.5% sodium deoxycholate, 1 U·mL^{-1} of benzonase (Sigma-Aldrich)], kept for 30 min on ice and centrifuged at 3000 g for 1 min. The supernatant from this step contained the nuclear fraction. All fractions were examined on western blots using polyclonal antibodies against individual organelle markers: for the cytosolic fraction, anti-α tubulin antibody (Sigma-Aldrich; #SAB3501071); for the microsomal fraction, anti-PDI antibody (Sigma-Aldrich; #P7496); and for the nuclear fraction, anti-histone H3 antibody (Merck Millipore, Burlington, MA, USA; #07-690). HBV proteins were immunoprecipitated as described above.

Co-immunoprecipitation and pull-down experiments

Cells co-transfected with either HBe-HA or HBe3CA-HA constructs and DNA encoding individual TRAP c-myc-tagged subunits were lysed 48 h after transfection for 1 h in Co-IP buffer (50 mM of HEPES, 100 mM of NaCl, 10% glycerol, 0.5% DOC, pH 7.9) supplemented with Complete™ EDTA-free protease-inhibitor cocktail (Roche). The lysates were cleared by centrifugation at 15 000 g for 10 min and subjected to immunoprecipitation using anti-HA magnetic beads at 4 °C for 2 h. The collected beads

were washed by Co-IP buffer without DOC. The samples were boiled in 2× sample buffer for 5 min to elute the proteins and analysed by SDS/PAGE followed by western blot using anti-c-myc antibody (Sigma-Aldrich; #C3956).

Liquid chromatography-tandem mass spectrometry analysis (LC-MS/MS)

Sample preparation has been described in detail previously [63]. Briefly, HBe-HA-producing cells were treated for 4 h with Brefeldin A (5 μg·mL^{-1}; Sigma-Aldrich) and harvested in lysis buffer containing 50 mM of Hepes, 100 mM of NaCl, 10% glycerol, and 0.5% Nonidet P40, pH 7.9. HA-tagged proteins were immunoprecipitated using anti-HA beads, washed, eluted by HA peptide (0.5 mg·mL^{-1}) and fragmented using chymotrypsin. The resulting peptides were separated on an UltiMate 3000 RSLCnano system (Thermo Fisher Scientific) coupled to an Orbitrap Fusion Lumos mass spectrometer (Thermo Fisher Scientific). The peptides were trapped and desalted with 2% acetonitrile in 0.1% formic acid at a flow rate of 30 μL·min^{-1} on an Acclaim PepMap100 column [5 μm, 5 mm by 300-μm internal diameter (ID); Thermo Fisher Scientific]. The eluted peptides were separated using an Acclaim PepMap100 analytical column (2 μm, 50 cm by 75 μm ID; ThermoFisher Scientific). The 125-min elution gradient at a constant flow rate of 300 nL·min^{-1} was set to 5% of phase B (0.1% of formic acid in 99.9% of acetonitrile) and 95% of phase A (0.1% of formic acid) for 1 min, after which the content of acetonitrile was gradually increased. The Orbitrap mass range was set from m/z 350 to 2000 in the MS mode, and the instrument acquired fragmentation spectra for ions of m/z 100–2000. A PROTEOME DISCOVERER 2.4 (ThermoFisher Scientific) was utilised for peptide and protein identification using Sequest and Amanda as search engines as well as databases of the sequences of HA-tagged HBe or HBe3CA, Swiss-Prot human proteins (downloaded on 15 February 2016), and common contaminants. The data were also searched with MAXQUANT (version 1.6.3.4; Max-Planck-Institute of Biochemistry, Planegg, Germany) and the same set of protein databases was applied to obtain peptide and protein intensities applied at the LFQ step. PERSEUS software (version 1.650; Max-Planck-Institute of Biochemistry) was used to perform LFQ comparison of three biological replicates of HA-tagged HBe (or HBe3CA) cells and three biological replicates of cells transfected with an empty vector. The data were processed to compare the abundance of individual proteins by statistical tests in the form of student's t-test and resulted in a volcano plot comparing the statistical significance and protein-abundance difference (fold change).

HBV-particle purification

HBV virions were produced in HepG2-hNTCP cells transfected with wt and C3A rcccDNA, as previously described

[64]. Briefly, rcccDNA for *wt* and mutant precore were transfected in triplicate into HepG2-hNTCP cells using Lipofectamine 3000 (ThermoFisher Scientific). The culture medium of transfected cells was collected every 3–4 days for the duration of 30 days. HBV particles were precipitated from clarified cell supernatants by overnight incubation in 6% polyethylene glycol 8000 (PEG 8000) and were then concentrated by centrifugation at 4 °C at 14 000 *g* for 90 min. The precipitated virions were re-suspended in complete DMEM supplemented with 10% FBS. HBV titres were determined by quantitative PCR (qPCR) using primers specific for HBV DNA: HBV-F, 5′-AGAGGACTCTTGGACTCTCTGC-3′; HBV-R, 5′-CTCCCAGTCTTTAAACAAACAGTC-3′; and the probe pHBV 5′-[FAM]TCAACGACCGACCTT[BHQ1]-3′. The qPCR reactions were performed with gb Elite PCR Master Mix (Generi Biotech, Hradec Kralove, Czech Republic) and a TaqMan probe.

HBV infection and the analysis of HBeAg and HBsAg by ELISA

HepG2-hNTCP cells were infected with *wt* and C3A mutant HBV in a 12-well plate format. The MOI was 2000 viral-genome equivalents per cell. The infection was performed overnight in the presence of 4% PEG8000, 2.5% DMSO and 3% FBS. The following day, the cells were washed three times with PBS and supplemented with fresh DMEM containing 2.5% DMSO and 3% FBS. The progress of HBV replication was checked by evaluating the titres of HBe and HBs antigens in culture supernatants using a commercial ELISA kit (Bioneovan, Beijing, China). Day 0 was defined as the time point when the viral inoculum was washed away and the fresh medium was added to the cells.

Statistical analysis

The numerical data of the evaluated intensity of the radioactive signal were analysed using two-tailed *t*-test (https://www.graphpad.com/quickcalcs/ttest1/), $n = 3$, significance level $\alpha = 0.05$. To compare the differences between experimental groups and control (ELISA), we performed an analysis of variance test (ANOVA) using GRAPHPAD PRISM v.6.05 (GraphPad Software, San Diego, CA, USA).

Acknowledgements

Conflict of interest

The authors declare no conflict of interest.

Author contributions

HZ and IP conceptualised the study. HZ, AZ, JH and BL investigated the study. HZ, AZ, BL, MH, AK and JW performed formal analysis. HZ, AZ and BL wrote the original draft. JW and IP wrote, reviewed and edited the manuscript. JW and IP performed funding acquisition.

Peer review

The peer review history for this article is available at https://publons.com/publon/10.1111/febs.16304.

Data availability statement

The mass spectrometry proteomics data have been deposited to the ProteomeXchange Consortium via the PRIDE [65] partner repository with the dataset identifier PXD025430 and https://doi.org/10.6019/PXD025430.

References

1 Ganem D & Varmus HE (1987) The molecular biology of the hepatitis B viruses. *Annu Rev Biochem* **56**, 651–693.

2 Nassal M & Schaller H (1993) Hepatitis B virus replication. *Trends Microbiol* **1**, 221–228.

3 Ou JH (1997) Molecular biology of hepatitis B virus e antigen. *J Gastroenterol Hepatol* **12**, S178–S187.

4 Chen M, Sällberg M, Hughes J, Jones J, Guidotti LG, Chisari FV, Billaud J-N & Milich DR (2005) Immune tolerance split between hepatitis B virus precore and core proteins. *J Virol* **79**, 3016–3027.

5 Milich D & Liang TJ (2003) Exploring the biological basis of hepatitis B e antigen in hepatitis B virus infection. *Hepatology* **38**, 1075–1086.

6 Milich DR, Chen MK, Hughes JL & Jones JE (1998) The secreted hepatitis B precore antigen can modulate the immune response to the nucleocapsid: a mechanism for persistence. *J Immunol* **160**, 2013–2021.

7 Ou JH, Laub O & Rutter WJ (1986) Hepatitis B virus gene function: the precore region targets the core antigen to cellular membranes and causes the secretion of the e antigen. *Proc Natl Acad Sci USA* **83**, 1578–1582.

8 DiMattia MA, Watts NR, Stahl SJ, Grimes JM, Steven AC, Stuart DI & Wingfield PT (2013) Antigenic switching of hepatitis B virus by alternative dimerization of the capsid protein. *Structure* **21**, 133–142.

9 Nassal M & Rieger A (1993) An intramolecular disulfide bridge between Cys-7 and Cys61 determines the structure of the secretory core gene product (e antigen) of hepatitis B virus. *J Virol* **67**, 4307–4315.

10 Selzer L, Katen SP & Zlotnick A (2014) The hepatitis B virus core protein intradimer interface modulates capsid assembly and stability. *Biochemistry* **53**, 5496–5504.

11 Jean-Jean O, Salhi S, Carlier D, Elie C, De Recondo AM & Rossignol JM (1989) Biosynthesis of hepatitis B virus e antigen: directed mutagenesis of the putative aspartyl protease site. *J Virol* **63**, 5497–5500.

12 Standring DN, Ou JH, Masiarz FR & Rutter WJ (1988) A signal peptide encoded within the precore region of hepatitis B virus directs the secretion of a heterogeneous population of e antigens in *Xenopus* oocytes. *Proc Natl Acad Sci USA* **85**, 8405–8409.

13 Ito K, Kim K-H, Lok AS-F & Tong S (2009) Characterization of genotype-specific carboxyl-terminal cleavage sites of hepatitis B virus e antigen precursor and identification of furin as the candidate enzyme. *J Virol* **83**, 3507–3517.

14 Messageot F, Salhi S, Eon P & Rossignol J (2003) Proteolytic processing of the hepatitis B virus e antigen precursor. *J Biol Chem* **278**, 891–895.

15 Chen MT, Billaud J-N, Sällberg M, Guidotti LG, Chisari FV, Jones J, Hughes J & Milich DR (2004) A function of the hepatitis B virus precore protein is to regulate the immune response to the core antigen. *Proc Natl Acad Sci USA* **101**, 14913–14918.

16 Riordan SM, Skinner N, Kurtovic J, Locarnini S & Visvanathan K (2006) Reduced expression of toll-like receptor 2 on peripheral monocytes in patients with chronic hepatitis B. *Clin Vaccine Immunol* **13**, 972–974.

17 Visvanathan K, Skinner NA, Thompson AJV, Riordan SM, Sozzi V, Edwards R, Rodgers S, Kurtovic J, Chang J, Lewin S *et al.* (2007) Regulation of Toll-like receptor-2 expression in chronic hepatitis B by the precore protein. *Hepatology* **45**, 102–110.

18 Lang T, Lo C, Skinner N, Locarnini S, Visvanathan K & Mansell A (2011) The hepatitis B e antigen (HBeAg) targets and suppresses activation of the toll-like receptor signaling pathway. *J Hepatol* **55**, 762–769.

19 Kimura T, Ohno N, Terada N, Rokuhara A, Matsumoto A, Yagi S, Tanaka E, Kiyosawa K, Ohno S & Maki N (2005) Hepatitis B virus DNA-negative dane particles lack core protein but contain a 22-kDa precore protein without C-terminal arginine-rich domain. *J Biol Chem* **280**, 21713–21719.

20 Hong X, Luckenbaugh L, Perlman D, Revill PA, Wieland SF, Menne S & Hu J (2021) Characterization and application of precore/core-related antigens in animal models of hepatitis B virus infection. *Hepatology* **74**, 99–115.

21 Hong X, Luckenbaugh L, Mendenhall M, Walsh R, Cabuang L, Soppe S, Revill PA, Burdette D, Feierbach B, Delaney W *et al.* (2021) Characterization of hepatitis B precore/core-related antigens. *J Virol* **95**, e01695-20.

22 Garcia PD, Ou JH, Rutter WJ & Walter P (1988) Targeting of the hepatitis B virus precore protein to the endoplasmic reticulum membrane: after signal peptide cleavage translocation can be aborted and the product released into the cytoplasm. *J Cell Biol* **106**, 1093–1104.

23 Ou JH, Yeh CT & Yen TS (1989) Transport of hepatitis B virus precore protein into the nucleus after cleavage of its signal peptide. *J Virol* **63**, 5238–5243.

24 Duriez M, Rossigno JM & Sitterlin D (2008) The hepatitis B virus precore protein is retrotransported from endoplasmic reticulum (ER) to cytosol through the ER-associated degradation pathway. *J Biol Chem* **283**, 32352–32360.

25 Deroubaix A & Kramvis A (2021) In vitro expression of precore proteins of hepatitis B virus subgenotype A1 is affected by HBcAg, and can affect HBsAg secretion. *Sci Rep* **11**, 8167.

26 Scaglioni PP, Melegari M & Wands JR (1997) Biologic properties of hepatitis B viral genomes with mutations in the precore promoter and precore open reading frame. *Virology* **233**, 374–381.

27 Locarnini S, Shaw T, Dean J, Colledge D, Thompson A, Li K, Lemon SM, Lau GGK & Beard MR (2005) Cellular response to conditional expression of the hepatitis B virus precore and core proteins in cultured hepatoma (Huh-7) cells. *J Clin Virol* **32**, 113–121.

28 Inoue J, Krueger EW, Chen J, Cao H, Ninomiya M & McNiven MA (2015) HBV secretion is regulated through the activation of endocytic and autophagic compartments mediated by Rab7 stimulation. *J Cell Sci* **128**, 1696–1706.

29 Liu D, Cui L, Wang Y, Yang G, He J, Hao R, Fan C, Qu M, Liu Z, Wang M *et al.* (2016) Hepatitis B e antigen and its precursors promote the progress of hepatocellular carcinoma by interacting with NUMB and decreasing p53 activity. *Hepatology* **64**, 390–404.

30 Mitra B, Wang J, Kim ES, Mao R, Dong M, Liu Y, Zhang J & Guo H (2019) Hepatitis B virus precore protein p22 inhibits alpha interferon signaling by blocking STAT nuclear translocation. *J Virol* **93**, e00196-19.

31 Lang S, Pfeffer S, Lee PH, Cavalié A, Helms V, Förster F & Zimmermann R (2017) An update on Sec 61 channel functions, mechanisms, and related diseases. *Front Physiol* **8**, 1–22.

32 Alder NN, Shen Y, Brodsky JL, Hendershot LM & Johnson AE (2005) The molecular mechanisms underlying BiP-mediated gating of the Sec61 translocon of the endoplasmic reticulum. *J Cell Biol* **168**, 389–399.

33 Hamman BD, Hendershot LM & Johnson AE (1998) BiP maintains the permeability barrier of the ER membrane by sealing the lumenal end of the translocon pore before and early in translocation. *Cell* **92**, 747–758.

34 Haßdenteufel S, Johnson N, Paton AW, Paton JC, High S & Zimmermann R (2018) Chaperone-mediated Sec61 channel gating during ER import of small

precursor proteins overcomes Sec61 inhibitor-reinforced energy barrier. *Cell Rep* **23**, 1373–1386.

35 Fons RD, Bogert BA & Hegde RS (2003) Substrate-specific function of the translocon-associated protein complex during translocation across the ER membrane. *J Cell Biol* **160**, 529–539.

36 Pfeffer S, Burbaum L, Unverdorben P, Pech M, Chen Y, Zimmermann R, Beckmann R & Förster F (2015) Structure of the native Sec61 protein-conducting channel. *Nat Commun* **6**, 8403.

37 Hartmann E, Görlich D, Kostka S, Otto A, Kraft R, Knespel S, Bürger E, Rapoport TA & Prehn S (1993) A tetrameric complex of membrane proteins in the endoplasmic reticulum. *Eur J Biochem* **214**, 375–381.

38 Yang SQ, Walter M & Standring DN (1992) Hepatitis B virus p25 precore protein accumulates in *Xenopus* oocytes as an untranslocated phosphoprotein with an uncleaved signal peptide. *J Virol* **66**, 37–45.

39 Lubyová B & Weber J (2020) Posttranslational modifications of HBV core protein. *Acta Virol* **64**, 177–186.

40 Yeh CT & Ou JH (1991) Phosphorylation of hepatitis B virus precore and core proteins. *J Virol* **65**, 2327–2331.

41 Lainé S, Thouard A, Derancourt J, Kress M, Sitterlin D & Rossignol J-M (2003) In vitro and in vivo interactions between the hepatitis B virus protein P22 and the cellular protein gC1qR. *J Virol* **77**, 12875–12880.

42 Heger-Stevic J, Zimmermann P, Lecoq L, Böttcher B & Nassal M (2018) Hepatitis B virus core protein phosphorylation: identification of the SRPK1 target sites and impact of their occupancy on RNA binding and capsid structure. *PLoS Pathog* **14**, e1007488.

43 Nguyen D, Stutz R, Schorr S, Lang S, Pfeffer S, Freeze HH, Förster F, Helms V, Dudek J & Zimmermann R (2018) Proteomics reveals signal peptide features determining the client specificity in human TRAP-dependent ER protein import. *Nat Commun* **9**, 3765.

44 Ludgate L, Adams C & Hu J (2011) Phosphorylation state-dependent interactions of Hepadnavirus core protein with host factors. *PLoS One* **6**, e29566.

45 Selzer L, Kant R, Wang JC-Y, Bothner B & Zlotnick A (2015) Hepatitis B virus core protein phosphorylation sites affect capsid stability and transient exposure of the C-terminal domain. *J Biol Chem* **290**, 28584–28593.

46 Wittkop L, Schwarz A, Cassany A, Grün-Bernhard S, Delaleau M, Rabe B, Cazenave C, Gerlich W, Glebe D & Kann M (2010) Inhibition of protein kinase C phosphorylation of hepatitis B virus capsids inhibits virion formation and causes intracellular capsid accumulation. *Cell Microbiol* **12**, 962–975.

47 Liao W & Ou JH (1995) Phosphorylation and nuclear localization of the hepatitis B virus core protein:

significance of serine in the three repeated SPRRR motifs. *J Virol* **69**, 1025–1029.

48 Rabe B, Vlachou A, Pante N, Helenius A & Kann M (2003) Nuclear import of hepatitis B virus capsids and release of the viral genome. *Proc Natl Acad Sci USA* **100**, 9849–9854.

49 Lubyova B, Hodek J, Zabransky A, Prouzova H, Hubalek M, Hirsch I & Weber J (2017) PRMT5: a novel regulator of Hepatitis B virus replication and an arginine methylase of HBV core. *PLoS One* **12**, e0186982.

50 Li HC, Huang EY, Su PY, Wu SY, Yang CC, Lin YS, Chang WC & Shih C (2010) Nuclear export and import of human hepatitis B virus capsid protein and particles. *PLoS Pathog* **6**, e1001162.

51 Yeh CT, Hong LH, Ou JH, Chu CM & Liaw YF (1996) Characterization of nuclear localization of a hepatitis B virus precore protein derivative P22. *Arch Virol* **141**, 425–438.

52 Wasenauer G, Köck J & Schlicht HJ (1992) A cysteine and a hydrophobic sequence in the noncleaved portion of the pre-C leader peptide determine the biophysical properties of the secretory core protein (HBe protein) of human hepatitis B virus. *J Virol* **66**, 5338–5346.

53 Shaffer KL, Sharma A, Snapp EL & Hegde RS (2005) Regulation of protein compartmentalization expands the diversity of protein function. *Dev Cell* **9**, 545–554.

54 Levine CG, Mitra D, Sharma A, Smith CL & Hegde RS (2005) The efficiency of protein compartmentalization into the secretory pathway. *Mol Biol Cell* **16**, 279–291.

55 Rapoport TA (2007) Protein translocation across the eukaryotic endoplasmic reticulum and bacterial plasma membranes. *Nature* **450**, 663–669.

56 Bonardi F, Halza E, Walko M, Du Plessis F, Nouwen N, Feringa BL & Driessen AJM (2011) Probing the SecYEG translocation pore size with preproteins conjugated with sizable rigid spherical molecules. *Proc Natl Acad Sci USA* **108**, 7775–7780.

57 Arkowitz RA, Joly JC & Wickner W (1993) Translocation can drive the unfolding of a preprotein domain. *EMBO J* **12**, 243–253.

58 Hegde RS & Kang SW (2008) The concept of translocational regulation. *J Cell Biol* **182**, 225–232.

59 Kriegler T, Lang S, Notari L & Hessa T (2020) Prion protein translocation mechanism revealed by pulling force studies. *J Mol Biol* **432**, 4447–4465.

60 Kriegler T, Kiburg G & Hessa T (2020) Translocon-associated protein complex (TRAP) is crucial for co-translational translocation of pre-proinsulin. *J Mol Biol* **432**, 166694.

61 Guo X, Chen P, Hou X, Xu W, Wang D, Wang TY, Zhang L, Zheng G, Gao ZL, He CY *et al.* (2016) The recombind cccDNA produced using minicircle

technology mimicked HBV genome in structure and function closely. *Sci Rep* **6**, 25552.

62 Holden P & Horton WA (2009) Crude subcellular fractionation of cultured mammalian cell lines. *BMC Res Notes* **2**, 243.

63 Langerová H, Lubyová B, Zábranský A, Hubálek M, Glendová K, Aillot L, Hodek J, Strunin D, Janovec V, Hirsch I *et al.* (2020) Hepatitis B core protein is post-translationally modified through K29-linked ubiquitination. *Cells* **9**, 2547.

64 Ni Y, Sonnabend J, Seitz S & Urban S (2010) The pre-S2 domain of the hepatitis B virus is dispensable for infectivity but serves a spacer function for L-protein-connected virus assembly. *J Virol* **84**, 3879–3888.

65 Perez-Riverol Y, Csordas A, Bai J, Bernal-Llinares M, Hewapathirana S, Kundu DJ, Inuganti A, Griss J, Mayer G, Eisenacher M *et al.* (2019) The PRIDE database and related tools and resources in 2019: improving support for quantification data. *Nucleic Acids Res* **47**, D442–D450.